Article

"Ab initio" liquid water

LAASONEN, Kari, *et al*.

Abstract

An ab initio molecular dynamics simulation of liquid water has been performed using density functional theory in the Kohn–Sham formulation and a plane wave basis set to determine the electronic structure and the forces at each time step. For an accurate description of the hydrogen bonding in the liquid, it was necessary to extend the exchange functional with a term that depends on the gradient of the electron density. A further important technical detail is that supersoft pseudopotentials were used to treat the valence orbitals of the oxygen atoms in a plane wave expansion. The structural and dynamical properties of the liquid were found to be in good agreement with experiment. The ab initio molecular dynamics also yields information on the electronic structure. The electronic feature of special interest is the lowest unoccupied molecular orbital (LUMO) of the liquid which is the state occupied by a thermalized excess electron in the conductive state. The main result of calculating the liquid LUMO is that it is a delocalized state distributed over interstitial space between the molecules with a significant admixture of [...]

Reference

LAASONEN, Kari, *et al*. "Ab initio" liquid water. *Journal of Chemical Physics*, 1993, vol. 99, no. 11, p. 9080-9089

DOI : 10.1063/1.465574

"*Ab initio*" liquid water

K. Laasonen, M. Sprik, and M. Parrinello
IBM Research Division, Zurich Research Laboratory, 8803 Rüschlikon, Switzerland

R. Car
IRRMA, PHB-Ecublens, 1015 Lausanne, Switzerland and University of Geneva, Switzerland

(Received 7 July 1993; accepted 23 August 1993)

An *ab initio* molecular dynamics simulation of liquid water has been performed using density functional theory in the Kohn–Sham formulation and a plane wave basis set to determine the electronic structure and the forces at each time step. For an accurate description of the hydrogen bonding in the liquid, it was necessary to extend the exchange functional with a term that depends on the gradient of the electron density. A further important technical detail is that supersoft pseudopotentials were used to treat the valence orbitals of the oxygen atoms in a plane wave expansion. The structural and dynamical properties of the liquid were found to be in good agreement with experiment. The *ab initio* molecular dynamics also yields information on the electronic structure. The electronic feature of special interest is the lowest unoccupied molecular orbital (LUMO) of the liquid which is the state occupied by a thermalized excess electron in the conductive state. The main result of calculating the liquid LUMO is that it is a delocalized state distributed over interstitial space between the molecules with a significant admixture of the σ^* orbitals of the individual water molecules.

I. INTRODUCTION

Realistic simulation of the behavior of aqueous solutions is of crucial importance in chemistry, biology, and physics. The modeling of pure water based on effective[1,2] or *ab initio*[3] potentials has reached a high degree of sophistication. However, quantitatively accurate modeling of aqueous ionic solutions still presents severe problems (for examples of polarizable models of aqueous alkali halides see Refs. 4–6). Car and Parrinello have developed a molecular dynamics (MD) scheme[7] in which the interatomic forces are not preassigned before the MD run but are calculated in the Born–Oppenheimer (BO) approximation from accurate electronic structure calculations during the simulation. This scheme has proved to be accurate and reliable for many semiconducting and metallic systems (for a review see Refs. 8–11). It is therefore highly desirable to find out whether the Car–Parrinello (CP) scheme is sufficiently accurate to treat aqueous solutions, as this would circumvent the lengthy and often not very reliable parametrization of the potential.

A prerequisite to this admittedly ambitious goal is to assess the ability of density functional (DF) based *ab initio* MD to describe the properties of water and the subtleties of hydrogen bonding in disordered systems. To this end we have performed a CP simulation of water. This simulation makes use of some very recent technical developments that have been successfully tested on ice[12,13] and water clusters,[14,15] namely, supersoft pseudopotentials introduced by Vanderbilt[16] and the successful new gradient corrections to the local density approximation.[17,18] The Vanderbilt pseudopotential allows us to represent the electron valence orbital in terms of plane waves using a relatively small energy cutoff in the plane wave expansion.[19,20] Furthermore, gradient corrections have dramatically improved the description of hydrogen bonding in DF theory.[12–15,21] Our results are encouraging insofar as they show that DF is able to reproduce sufficiently well the main static and dynamical properties of water. However, we find some quantitative dependence of our results on the choice of the gradient corrections.

The CP scheme calculates the electronic structure self-consistently by adapting the electron wave functions to the evolving ionic configuration. Hence, chemical processes such as charge transfer or the formation and breaking of covalent bonds are, in principle, treated on the same level as the intermolecular interactions. It is, of course, this aspect that distinguishes the CP scheme from model-based simulations and which, hopefully, will ultimately enable us to study chemical reactions. One of the fields of research to which *ab initio* MD simulation can already contribute is the investigation of the ultrafast reaction dynamics following dissociation or ionization of an excited water molecule in the liquid.[22–26] The time scale of most relevant reaction processes is a few picoseconds and hence well within the range of an *ab initio* MD run on present-day workstations. Therefore, despite the drawback of being limited to adiabatic ground state dynamics, the *ab initio* MD approach can be useful in characterizing the various dissociation products and in exploring the reaction pathways and transition states in the adiabatic limit. Solvent effects, which play a major role in all of these complex phenomena, are automatically included in such simulations.

A characteristic and intensively studied photolysis product of water molecules in the liquid are excess electrons. Experiment[22–24] has established that the electrons are ejected into the conduction band where they are rapidly thermalized. In the next period of 0.2 to 0.5 ps, the delocalized state decays into the cavity state of the solvated electron. Experiment[22–24] as well as model-based computer simulation studies[25,26] indicate that complete solvation proceeds through one or more intermediate states. Direct in-

 0021-9606/93/99(11)/9080/10/$6.00

vestigation by *ab initio* MD of the solvated electron or its various precursors is, at the present stage, prohibited by limitations of system size. However, the initial delocalized state before it has induced any reconstruction in the liquid can be studied in a relatively small water sample under periodic boundary conditions. Hence, we will use our first *ab initio* MD simulation of water to examine the lowest unoccupied molecular orbital (LUMO) of pure water and to draw a comparison between it and the excess electron in the conductive state.

The paper is organized as follows: In Sec. II we describe the CP method, in Sec. III the Vanderbilt pseudopotential. Section IV is devoted to describing the gradient-corrected DF. Sections V, VI, and VII describe our results for the atomic and electronic properties of water. The conclusion and final comments are to be found on Sec. VIII.

II. CAR–PARRINELLO METHOD

We use here the CP approach[7] to generate the BO dynamics. Details of the method can be found in Refs. 8–11; we will recall its basic principles here.

An extended Lagrangian is introduced in which the classical variables are the electronic wave functions $\phi_i(\mathbf{r})$ and the ionic coordinates $\mathbf{R}_I$

$$\mathscr{L}=\mu\sum_i\int d\mathbf{r}\,|\dot{\phi}_i(\mathbf{r})|^2+\sum_I\frac{1}{2}M_I\dot{\mathbf{R}}_I^2-E_{KS}(\{\phi_i,\mathbf{R}_I\}) \tag{1}$$

subject to the orthonormality constraints

$$\langle\phi_i|\phi_j\rangle=\delta_{ij}. \tag{2}$$

Here μ is a fictitious mass parameter for the electronic degrees of freedom, M_I is the mass of the atoms, E_{KS} is the total energy of the system. The orthonormality constraints are incorporated by introducing Lagrange multipliers Λ_{ij}. The equations of motion become

$$\mu\ddot{\phi}_i=-\frac{\delta E_{KS}}{\delta\phi_i^*}+\sum_j\Lambda_{ij}\phi_j, \tag{3}$$

$$M_I\ddot{\mathbf{R}}_I=-\frac{\partial E_{KS}}{\partial\mathbf{R}_I}. \tag{4}$$

The dynamics that follows from these equations of motion has been analyzed several times. It has been shown that under appropriate conditions it closely approximates the BO dynamics, namely the dynamics imposed by the Hellman–Feynman forces

$$\mathbf{F}_I=-\frac{\partial E_{KS}}{\partial\mathbf{R}_I}, \tag{5}$$

where the derivatives are calculated using the ground state wave functions that correspond to the instantaneous ionic configuration $\{\mathbf{R}_I\}$. Crucial to the practical success of this approach has been the use of the Kohn–Sham scheme to obtain the ground state energy and the expansion of the electronic orbitals $\phi_i(\mathbf{r})$ into plane waves. However, this basis set is very inefficient for describing the rapidly varying core electron orbitals. Hence, pseudopotentials are used to integrate out these degrees of freedom. Only the valence electrons are treated explicitly, the interaction between the valence electrons and the ionic cores now being described by potential functions.

The pseudopotential scheme when combined with the Kohn–Sham version of the density functional theory (DFT) gives for the total energy of N_v valence electrons the following expression:

$$E_{KS}[\{\phi_i\},\{\mathbf{R}_I\}]=\sum_i\langle\phi_i|-\tfrac{1}{2}\nabla^2+V_{\mathrm{NL}}|\phi_i\rangle+\frac{1}{2}\int\int d\mathbf{r}\,d\mathbf{r}'\,\frac{\rho(\mathbf{r})\rho(\mathbf{r}')}{|\mathbf{r}-\mathbf{r}'|}+E_{\mathrm{xc}}[\rho]+\int d\mathbf{r}\,V_{\mathrm{loc}}^{\mathrm{ps}}(\mathbf{r})\rho(\mathbf{r})+U(\{\mathbf{R}_I\}), \tag{6}$$

where $\rho(\mathbf{r})$ is the electron density, E_{xc} is the exchange and correlation energy, and $U(\{\mathbf{R}_I\})$ is the ion–ion interaction energy. The pseudopotential contains two parts, a local part $V_{\mathrm{loc}}^{\mathrm{ps}}(\mathbf{r})=\Sigma_I V_{\mathrm{loc}}^{\mathrm{ion}}(|\mathbf{r}-\mathbf{R}_I|)$ and a nonlocal part for which several different expressions have been proposed.[27] The pseudopotential is constructed in such a way that the pseudowave functions match the all-electron valence wave functions outside a given core radius r_c for a reference atomic state, which is usually taken to be the ground state or a slightly excited atomic configuration. In order to satisfy the above requirement the integral of the square of the wave function inside a core sphere of radius r_c must be the same for the all-electron and the pseudowave function. This is the norm-conservation condition.[28] Norm conservation also guarantees that the behavior of the logarithmic derivative of the pseudowave function at r_c is similar to that of the all-electron wave function for small energy variations around an eigenvalue.[28] As a consequence norm-conserving pseudopotentials have good transferability properties, i.e., they preserve a good match between pseudo- and all-electron wave functions when the atom is placed in a condensed matter environment, i.e., in an environment different from the atomic reference state.

In the case of first-row elements such as O the standard procedure to construct norm-conserving pseudopotentials[28] leads to very hard pseudopotentials, and therefore a prohibitively large number of plane waves is needed to represent these rapid variations. Much effort has recently been devoted to remedy this situation. On the one hand, procedures have been devised that yield optimally smooth norm-conserving pseudopotentials.[29,30] Others have suggested[16,31] to generalize the pseudopotential concept in a way that allows the pseudowave functions to be augmented in the core region in the same spirit of linear augmented plane wave calculations.[32] This procedure requires releasing norm conservation. Pseudopotentials having equally good transferability properties as the norm-conserving pseudopotentials are generated at the price of an increased number of atomic reference states and of a more complicated nonlocal form of the pseudopotential. The advantage is that the number of plane waves needed to represent the pseudowave functions is considerably reduced even with

respect to optimally smooth norm-conserving pseudopotentials. For this reason we have chosen to use the Vanderbilt scheme[16] which is outlined in the following section. Pseudopotentials of this kind are referred to as supersoft.

III. THE VANDERBILT PSEUDOPOTENTIAL SCHEME

Vanderbilt has suggested[16] that the nonlocal part of the pseudopotential be written in the fully nonlocal form

$$V_{\mathrm{NL}}=\sum_{nm,I} D_{nm}^{(0)}|\beta_n^I\rangle\langle\beta_m^I|, \tag{7}$$

where the functions β_n^I span the core space and vanish outside it. The β_n^I functions characterize the pseudopotential together with the coefficients $D_{nm}^{(0)}$ and the local part. The corresponding pseudowave functions ϕ_i match the all-electron valence wave functions outside the core region, but, at variance with usual pseudowave functions, they do not satisfy the requirement of norm conservation. As a consequence one has to write the electron density as the sum of two terms, a smooth delocalized part given by the squared moduli of the pseudowave functions, and an *augmented* part localized in the core regions which is given in terms of functions $Q_{nm}(\mathbf{r})$

$$\rho(\mathbf{r})=\sum_i\left[\left|\phi_i(\mathbf{r})\right|^2+\sum_{nm,I} Q_{nm}^I(\mathbf{r})\langle\phi_i|\beta_n^I\rangle\langle\beta_m^I|\phi_i\rangle\right]. \tag{8}$$

The augmentation functions $Q_{nm}^I(\mathbf{r})=Q_{nm}(\mathbf{r}-\mathbf{R}_I)$ are also provided by the pseudopotential construction and are strictly localized in the core regions. Thus the electron density in Eq. (8) is still quadratic in the wave functions, but the definition of the density differs from the normal pseudopotential scheme. Now the density also depends explicitly on the ionic positions through the $Q_{nm}^I(\mathbf{r})$ functions.

Another consequence of relaxing the norm-conserving condition is a generalized orthonormality condition

$$\langle\phi_i|S(\{\mathbf{R}_I\})|\phi_j\rangle=\delta_{ij}, \tag{9}$$

where S is an overlap operator given by

$$S=1+\sum_{nm,I} q_{nm}|\beta_n^I\rangle\langle\beta_m^I| \tag{10}$$

and $q_{nm}=\int d\mathbf{r}\, Q_{nm}(\mathbf{r})$. The orthonormality condition (9) is consistent with the conservation of the charge $\int d\mathbf{r}\, n(\mathbf{r})=N_v$. Note that the overlap operator S is also dependent on the ionic positions through the $\beta_n^I(\mathbf{r})$ functions. The use of generalized orthonormality constraints that depend on the ionic positions require some modification of the CP equations (4), which now read[20]

$$\mu\ddot{\phi}_i=-\frac{\delta E_{KS}}{\delta\phi_i^*}+\sum_j \Lambda_{ij}S\phi_j, \tag{11}$$

$$M_I\ddot{\mathbf{R}}_I=-\frac{\partial E_{KS}}{\partial\mathbf{R}_I}+\sum_{ij}\Lambda_{ij}\left\langle\phi_i\left|\frac{\partial S}{\partial\mathbf{R}_I}\right|\phi_j\right\rangle. \tag{12}$$

Finally, to be able to perform the MD simulation, one has to know the forces in Eqs. (11) and (12) and solve for the Lagrange multipliers. The values of Λ_{ij} are determined using a SHAKE-type method.[20,33] The forces can be relatively easily derived as partial derivatives of E_{KS}. The derivatives with respect to the electronic orbitals are

$$\frac{\delta E_{KS}}{\delta\phi_i^*(\mathbf{r})}=[-\tfrac{1}{2}\nabla^2+V_{\mathrm{eff}}(\mathbf{r})]\phi_i(\mathbf{r})+\sum_{nm,I} D_{nm}^I\langle\mathbf{r}|\beta_n^I\rangle\times\langle\beta_m^I|\phi_i\rangle, \tag{13}$$

where

$$V_{\mathrm{eff}}(\mathbf{r})=V_{\mathrm{loc}}^{\mathrm{ps}}(\mathbf{r})+\int d\mathbf{r}'\frac{n(\mathbf{r}')}{|\mathbf{r}-\mathbf{r}'|}+\frac{\delta E_{\mathrm{xc}}[n]}{\delta n(\mathbf{r})},$$
$$D_{nm}^I=D_{nm}^{(0)}+\int d\mathbf{r}\, V_{\mathrm{eff}}(\mathbf{r})Q_{nm}^I(\mathbf{r}), \tag{14}$$

and those with respect to the ionic coordinates

$$\frac{\partial E_{\mathrm{tot}}}{\partial\mathbf{R}_I}=-\frac{dU}{d\mathbf{R}_I}-\int d\mathbf{r}\frac{dV_{\mathrm{loc}}^{\mathrm{ps}}}{d\mathbf{R}_I}n(\mathbf{r})-\sum_{nm}D_{nm}^I\frac{\partial\rho_{nm}^I}{\partial\mathbf{R}_I}-\int d\mathbf{r}\, V_{\mathrm{eff}}(\mathbf{r})\sum_{nm}\rho_{nm}^I\frac{dQ_{nm}^I}{d\mathbf{R}_I}, \tag{15}$$

where $\rho_{nm}^I=\Sigma_i\langle\phi_i|\beta_n^I\rangle\langle\beta_m^I|\phi_i\rangle$.

In an MD implementation it is crucial that the derivative shown in Eq. (15) is really the exact (partial) derivative of E_{KS}. To obtain exact derivatives in other basis sets or with other methods is usually much more difficult. This feature is one of the reasons for the success of the plane wave-based CP method.

IV. ROLE OF THE EXCHANGE AND CORRELATION FUNCTION

In DF theory the exchange and correlation energy is expressed as a functional of the density $E_{\mathrm{xc}}[\rho]$.[34] As the exact form of this functional is unknown, some approximation has to be used. One of the simplest approximations, the local density approximation (LDA), has proven to be very reliable for many covalently bonded materials and metals. The LDA assumes that the xc energy depends only on the value of the density at each point. The density-to-energy function is obtained by interpolating[35] the results of a quantum Monte Carlo calculation of the homogeneous electron gas.[36] The LDA typically overestimates the binding energy significantly, but yields very good bond lengths and vibrational frequencies in the case of covalent or metallic bonding.[34] But in the case of weakly bonded systems, like hydrogen or van der Waals,[37] the LDA fails badly. For example LDA gives a binding energy for the water dimer that is 60% too high and an O–O distance that is 10% too short.[14] The LDA would also predict the ice X to be metastable at 0 pressure, while the experimental pressure at that density would be ~80 GPa.[13] These errors are so large that some correction to LDA has to be made.

Several approaches have been proposed to correct LDA. We use here generalized gradient corrections (GC) where the xc energy also depends on gradients of the density.[38] The explicit form of the exchange part is from Becke,[17]

$$E_x^{GC} = -b \sum_\sigma \int dr\, \rho_\sigma^{4/3} \frac{x_\sigma^2}{1+6bx_\sigma \sinh^{-1}(x_\sigma)}, \quad (16)$$

where b has the value 0.0042 a.u., ρ_σ is the *spin* density and $x_\sigma = |\nabla\rho_\sigma|/\rho_\sigma^{4/3}$. (Note that here $\rho_\sigma = 1/2\rho$.)

The correction to the correlation is from Perdew,[18]

$$E_c^{GC} = \int dr\, e^{-\Phi(\rho)} C(\rho) \rho(\mathbf{r})^{-4/3}, \quad (17)$$

where

$$C(\rho) = a_1 + \frac{a_2 + a_3 r_s + a_4 r_s^2}{1 + a_5 r_s + a_6 r_s^2 + 10^4 a_4 r_s^3},$$
$$\Phi(\rho) = 0.191\,95[C(\infty)/C(\rho)]\,|\nabla\rho|\,\rho^{-7/6}, \quad (18)$$

and $\rho = (4\pi r_s^3/3)^{-1}$, $a_1 = 0.001\,667$, $a_2 = 0.002\,568$, $a_3 = 0.023\,266$, $a_4 = 7.389 \times 10^{-7}$, $a_5 = 8.723$, $a_6 = 0.472$ in atomic units.

This GC scheme has been shown to give a good description of H bonding in the water dimer,[14] in small water clusters,[15] in ice X[12] and ice Ic.[13] In other systems these gradient corrections also significantly improve the binding energies[37–39] and to a lesser extent the structural properties. In order to implement the GC scheme within our MD approach based on PW we faced severe difficulties related to the use of truncated Fourier expansions. Our way of dealing with these problems is described in the Appendix.

V. SIMULATION DETAILS

We have simulated a system of 32 D_2O molecules contained in a cubic cell of length 9.6 Å with periodic boundary conditions at room temperature. This amounts to a density equal to the experimental one. As discussed above, in order to make this calculation feasible it is necessary to use the supersoft pseudopotential scheme of Vanderbilt. The pseudopotential of oxygen has been generated following the prescription of Vanderbilt and with a core radius of 0.74 Å and two reference energies per angular momentum channel. The reference energies were chosen to be the $2s$ and $2p$ eigenvalues of oxygen ($\epsilon_s = -1.76$ Ry and $\epsilon_p = -0.67$ Ry).[19] In the construction of the pseudopotential the GC density functional has been applied consistently. In order to remove the $1/r$ singularity and thus accelerate the convergence with the energy cutoff, we have also constructed a pseudopotential for H. The Vanderbilt scheme was used here as well and the GC were consistently incorporated in the generation procedure. The pseudopotential for H contained only one s-symmetry function and the core radius was 0.37 Å.

The time step for the simulation was 0.169 fs and the μ parameter in the Lagrangian was $\mu = 1100$ a.u. In order to be able to use such a large value of μ and thus a relatively large time step we were forced to use D_2O rather than ordinary water in order to ensure an adiabatic decoupling of the electron and ionic motion. The choice of D_2O has the added benefit that quantum effects on the ionic motions are less important in D_2O. Since these are completely neglected in our calculation, comparison with experiments is easier. Furthermore, some of the experimental data such as neutron diffraction are available only for the deuterated species.

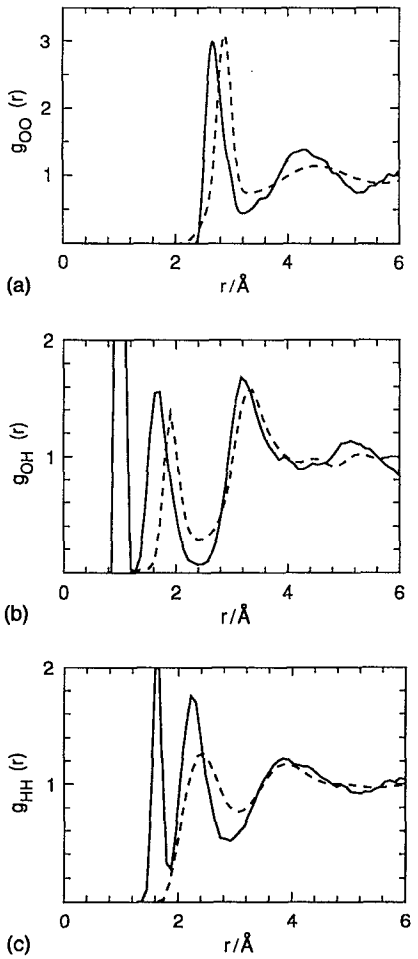

FIG. 1. The partial radial distribution functions of water. The solid line represents the results from the *ab initio* MD simulation with the full Becke–Perdew gradient corrections (see the text); the dashed lines are the experimental results from Ref. 41.

We first performed a run using the Becke–Perdew (BP) GC density functional. The initial configuration was taken from an equilibrated MD run which used the TIP4P interaction site potential.[40] After an equilibration time of 0.5 ps we collected statistics for a total duration of 1.5 ps. This time is long compared to the librational motion and comparable to the slowest vibrational times in liquid water. The results for the pair correlation are shown in Fig. 1 and compared with experimental data.[41] The overall agreement is satisfactory, but the O–O separation is too short. The theoretical value is 2.69 Å while the experimental value is 2.87 Å which constitutes an error of 6%. Similar shifts are seen in $g_{OH}(r)$ and $g_{HH}(r)$. Another general defect of the theoretical $g_{ij}(r)$ is that they appear overstructured, the secondary peaks exhibiting oscillations that are much too strong. All these features are probably the result of too short a hydrogen bond. The tendency of the BP exchange and correlation to give a short O–O bond was already observed in Ref. 15, where it was also seen that this ten-

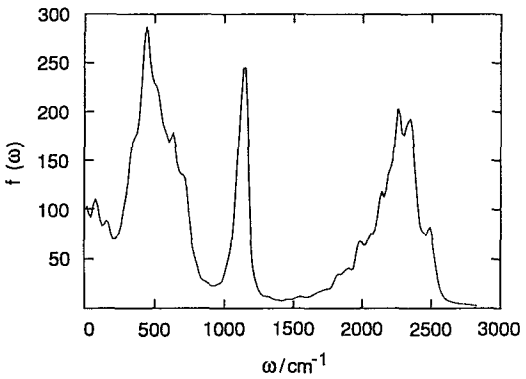

FIG. 2. The spectral density of the velocity autocorrelation of liquid (heavy) water.

dency was compounded by a collective effect when one goes from the dimer to the larger clusters.

We have also investigated some dynamical properties. The system showed normal liquidlike behavior and the diffusion coefficient measured from the Einstein relation was $D=(2.2\pm 1)10^{-5}$ cm^2 s^{-1} to be compared with the experimental value of $D=2.4\times 10^{-5}$ cm^2 s^{-1}.[42] Such an excellent agreement is somewhat coincidental, considering the very short duration of the run. However, we find it rewarding that our diffusion coefficient is in the correct range. We have also studied some of the vibrational properties through the calculation of the velocity–velocity autocorrelation spectrum

$$C_{vv}(\omega)=\sum_I \int dt[\mathbf{V}_I(t)\cdot\mathbf{V}_I(0)]e^{i\omega t}. \tag{19}$$

The spectrum obtained for our D_2O sample is shown in Fig. 2. Three broad peaks are observed at $\omega=2300$, 1100, and 500 cm^{-1}. They correspond to the D–O stretching mode, the bending mode, and the librational and vibrational modes. Owing to interaction these peaks are broadened. Correcting our results for the mass differences, we find for H_2O the stretching and librational modes $\omega=3200$, 1600, and 800 cm^{-1}, which are in good agreement with experiment (for a review of optical experiments see Ref. 43, for inelastic neutron scattering see, e.g., Ref. 44) Line shapes and band widths are also semiquantitatively correct.

VI. EFFECT OF A DIFFERENT GRADIENT CORRECTION

Most of the calculations reported here are based on the GC of BP. However, at present GC are not as well established as the local density part. In particular, we notice that a good description of exchange effects is crucial for a good description of hydrogen bonding, as shown by Hartree–Fock calculations on small water clusters.[45,46] The generalized gradient corrections, for exchange due to Becke, have been empirically adjusted to reproduce the exchange energies of atoms and have been shown to improve the LDA description of chemical bonding on a large molecular data base.[17]

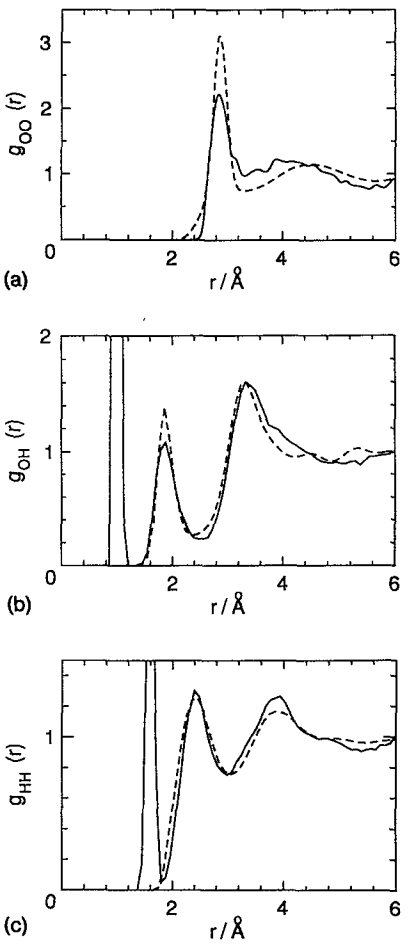

FIG. 3. The partial radial distribution functions of water. The solid line represents the results from the *ab initio* MD simulation with the Becke gradient correction for exchange only; the dashed lines are the experimental results from Ref. 41 (from Ref. 47).

Therefore we decided to perform a simulation using only the exchange corrections of Becke in order to assess the uncertainties associated with the choice of the GC. Thus the Perdew term was omitted from the GC functional and the pseudopotential was recalculated accordingly. The E_{xc}^{B} simulation is a continuation of the E_{xc}^{BP} trajectory from which the final configuration was taken as the starting point. The temperature was increased to 400 K for the initial 0.3 ps in order to accelerate memory loss. Next, the system was equilibrated again for 1.5 ps at 300 K. The results of the final averaging run of 2 ps are depicted in Fig. 3, which shows a great improvement in the peak position and in the quality of the $g(r)$. This is certainly very encouraging. However, we feel that more extensive tests on a variety of systems are necessary to obtain reliable GC functionals.[38]

VII. ELECTRONIC PROPERTIES

A special feature of the CP and related approaches is the insight they can provide into the electronic properties. We have taken advantage of this by investigating a few properties related to electronic states.

TABLE I. Various properties of water.

	LDA+GC	Expt.
Monomer		
μ (D)	1.86	1.855[a]
HOMO-LUMO gap (eV)	6.7	
Ionization energy	~12 eV	12 eV[b]
Dimer		
HOMO-LUMO gap (eV)	5.4	
Ionization energy	~12eV	
Liquid		
$D(10^{-9}m^2 s^{-1})$	2.2 ±1	2.4[c]
μ_{ave} (D)	2.66±0.04	2.6[d]
HOMO-LUMO gap (eV)	4.6 ±0.05	9.8[e]

[a]From Ref. 48.
[b]From Ref. 51.
[c]From Ref. 42.
[d]From Ref. 49.
[e]From Refs. 50, 54, and 55, see the text.

One of the simple yet crucial properties is the value of the dipole moment in water. This is experimentally known to vary from 1.855 D (Ref. 48) to 2.5–2.6 D in going from the gas to the condensed phase.[49] A correct value of the dipole moment is a necessary prerequisite for a realistic description of H_2O dielectric properties,[2] a crucial quantity in many solvation processes. The change in the dipole moment μ in going from the gas to the condensed phases cannot be reproduced by empirical models unless they explicitly take electronic polarizability into account.[2,3] In the CP approaches this is automatically taken into account and thus the value of the enhancement of the dipole moment can be extracted from our calculation.

We evaluate the average value of μ from the expression

$$\mu=\frac{1}{N}\sum_I \int d\Omega \int_0^{R_m} dr\, r^2 \mathbf{r}\rho(\mathbf{r}-\mathbf{R}_I), \tag{20}$$

where $\rho(\mathbf{r}-\mathbf{R}_I)$ is the total charge density (electrons +ions) associated with molecule I, the sum runs over all the N molecules in the system and $\mathbf{R}_I$ is the center of the ionic charges for the Ith molecule. Clearly the value of μ depends on the choice of R_m which we have set to R_m =1.32 Å, which is half the average O–O bonding length. With this value of R_m, we obtain μ=2.66 D, while variations of R_m of ±0.05 Å induced variations of μ of ±0.04 D. This relatively minor sensitivity to the choice of R_m makes us confident of the soundness of our estimate. The results for the dipole moment and other relevant properties are summarized in Table I along with the experimental data. The value obtained for μ is in reasonable agreement with experimental findings.[49] In Ref. 2 it is shown that this value is also consistent with the experimentally observed dielectric constant. This will open the way for *ab initio* simulations of ionic solutions where a correct description of electronic polarizability is crucial, as recently emphasized in Refs. 4–6.

We have also monitored the distribution of the Kohn–Sham eigenvalues for the occupied and for some of the unoccupied levels (the manifold of levels at the highest energy is unreliable since not all unoccupied states have been taken into account). In Fig. 4 we show the full density of states in the liquid. Figure 5 is a schematic representation that compares the electronic spectrum in the liquid to the energy level structure of the H_2O molecule and its dimer. Intermolecular interactions induce significant broadening of the energy levels relative to the isolated molecule. The lower levels remain largely unmodified, while larger effects are seen for higher levels. It is to be noted that the broadening in the condensed phase is very well comparable to the level splittings that are observed in going from the isolated molecule to the dimer.

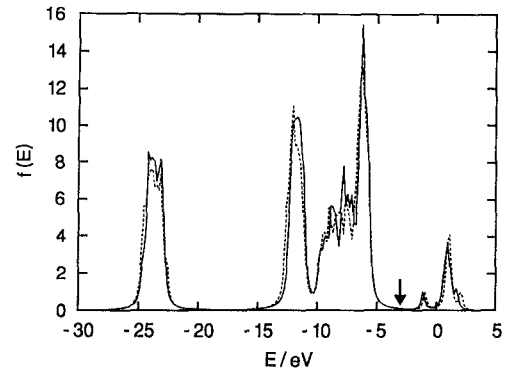

FIG. 4. Electronic density of states of liquid water. The solid and dashed curves are the distribution of single electron energies for two water configurations sampled from the *ab initio* MD run at a time interval of 1 ps. The separation between occupied and unoccupied states (Fermi energy) is indicated by an arrow. From Ref. 47.

Another conclusion that can be drawn from Figs. 4 and 5 is that the broad manifold starting at −10 eV and terminating with a sharp peak of highest occupied molecular orbital (HOMO) states at −6 eV is composed of a mixture of the $3A_1$ bonding and $1B_1$ lone pair oribitals. Photoelectron spectroscopy (PES) experiments determine the HOMO levels at −11 eV.[50] The discrepancy with the KS value of −6 eV in Fig. 4 is an indication of the difficulty of determining absolute energies (i.e., the location of

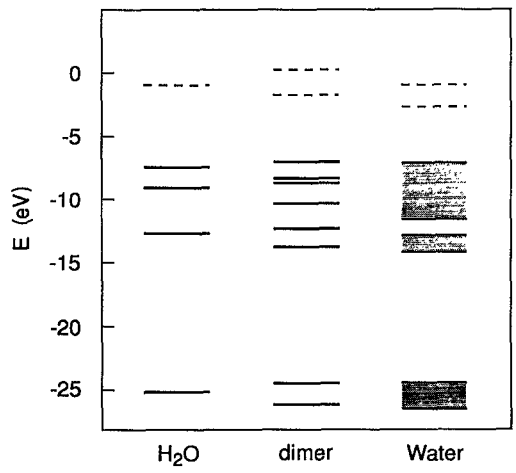

FIG. 5. Energy level diagram comparing the Kohn–Sham energies of the water monomer (left) and the dimer (middle) to the electronic density of states in the liquid (right) of Fig. 4.

the vacuum). Energy differences, on the other hand, are more reliable. Thus comparing the energies of the positive ion with that of the neutral molecule (ignoring the complications introduced by the periodic boundary conditions) we obtain a value of ~12 eV which is in good agreement with the experimental value of 12.6 eV[51] and the HF-STO estimate of 13.8 eV.[52]

Before considering the unoccupied levels in Fig. 4, it should be recalled that DF and HF are, strictly speaking, theories for the ground state energy, and as such they are not expected to provide accurate information on the energy levels. However, experience has shown that in spite of these shortcomings DFT is capable of describing the nature of the LUMO rather well, provided the LUMO is stable. For closed-shell molecules such as water, the LUMO is generally in the continuum and hence unstable. Therefore, the values of the HOMO-LUMO gap of the monomer and dimer in Fig. 5 (see also Table I) are not very meaningful. The apparent stability of these orbitals can be the result of a variety of effects such as periodic boundary conditions.

The energy difference which separates the occupied molecular orbitals and the manifold of empty states in the liquid is found to be 4.6 eV. Contrary to the HOMO-LUMO splitting of the monomer and dimer, this number is significant and is similar to a band gap in a solid. In the condensed phase the average spacing of the molecules is imposed by the density. Hence, in the liquid simulation the periodic boundaries are no longer arbitrary but determined by the number of particles and the density. A direct comparison with an experimental conduction band gap in water (or ice) is not straightforward since the electronic ice spectrum is dominated by electron–hole pairs.[50,53] For example, the maximum seen at 8.3 eV is most likely an exciton of molecular origin.[53] It is possible, however, to obtain an indirect estimate of the band gap using the minimum energy of delocalized states V_0 in water as obtained from work function measurements. Although the determination of V_0 has been subject to some debate, studies of ice–vacuum[54] and metal electrode–water[55] interfaces seem to converge on a value of $V_0 = -1.2$ eV. Subtracting from this number the PES energy (-11 eV) of the HOMO levels, we obtain a value of 9.8 eV for the experimental band gap, which is larger than our theoretical estimate by a factor of 2. This ratio is typical for DFT; thus water confirms a trend observed in many semiconducting systems and insulators.

Bearing in mind that the LUMO levels of H_2O and $(H_2O)_2$ are somewhat artificial, it is nonetheless instructive to examine the nature of these states more closely. In fact, the replication of the clusters by the periodic boundary conditions in our approach amounts to having a system with a low but finite density. The monomer and dimer levels can be thought of as evolving from the liquid water LUMO with decreasing density. The LUMO of a single H_2O molecule shown in Fig. 6 is the σ^* LUMO which is also found in HF calculations with a restricted basis set. It is an A_1 state. The main features of this molecular orbital are the presence of a significant probability density in the proximity of the O and two lobes that protrude rather far

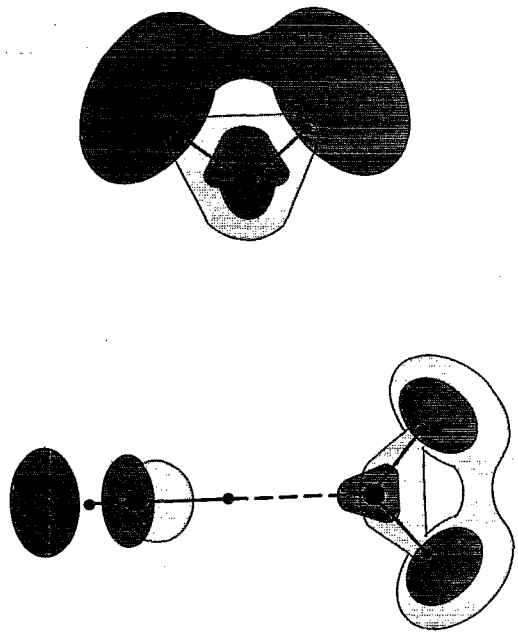

FIG. 6. Schematic representation of the LUMO (dark gray) for the H_2O monomer (top) and dimer (bottom). The light gray areas indicate the extension of charge density of the occupied states for the monomer. For the dimer they give an impression of the LUMO+1. From Ref. 47.

from the molecule in the H directions. The nature of the dimer LUMO is not very surprising, it being the σ^* state of the acceptor molecule (see Fig. 6). The LUMO+1 state is more interesting, one striking feature being the much reduced amplitude at the hydrogen bond. Both orbitals also have substantial amplitudes close to the O atoms of the two molecules and are quite extended.

The characterization of the LUMO in the weakly coupled low density limit is helpful for the analysis of the LUMO in the liquid under conditions of stronger interactions. This is the state (or band of states) that will be occupied by an excess electron just after injection in the liquid (prior to solvation). The hydrated electron has been studied by various groups.[25,26,56–59] These studies treat only the excess electron and use pseudopotentials of different complexity in order to describe the interaction between this single electron and the water molecules.[56–58] The main physical effect taken into account by these pseudopotentials is the excluded volume due to the closed electronic shells of the water molecules and the long-range electrostatic attraction due the polar OH bonds (in addition, some potentials also include polarization effects[57,59]). For the electron in the unreconstructed liquid, this leads to a delocalized scattering state where the electronic wave function is repelled by the molecules.[26] The corresponding eigenvalue is pushed up in energy relative to the vacuum level due to the reduced volume accessible to the electron. The attractive electrostatic energy is not sufficient to compensate for the increase in kinetic energy. The resulting V_0 value is positive contrary to experiment (see discussion above).

This picture, however, is somewhat controversial since quantum mechanical calculations on $e^-(H_2O)_6$ clusters

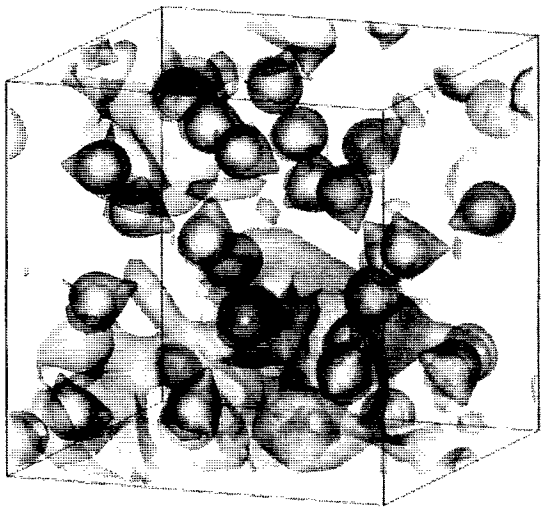

FIG. 7. The "LUMO" state of water. The heart-shaped objects are equidensity surfaces of the total density [$\rho(\mathbf{r})=0.1$ e/(a.u.)^3] and correspond to single molecules. The diffuse surface is the equidensity surface corresponding to the LUMO state [$\rho_i(\mathbf{r})=0.002$ e/(a.u.)^3] with compact pockets inside the molecules.

indicate a participation of the excess electronic state in the σ^* orbital of the molecule.[60,61] Spin echo experiments[62] have been interpreted along the same lines. We show in Fig. 7 the probability density associated with the water LUMO for a given molecular configuration. Two features are evident: The state is rather delocalized and there is some probability density close to the O. This is an indication of a sizable σ^* component. We can make these two statements quantitative by looking at the participation ratio p

$$p=\frac{1}{V\int d\mathbf{r}\,|\psi^*(\mathbf{r})\psi(\mathbf{r})|^2}, \tag{21}$$

which gives a measure of the degree of localization. The participation ratio goes from $p=1$ for an infinitely extended plane wave state to $p\sim 1/V$ where V is the volume of the system in the case of a point like localization. In the Vanderbilt scheme, because of the relaxation of the norm conservation, Eq. (21) has to be rewritten

$$p=\frac{1}{V\int d\mathbf{r}\,|\psi^*(\mathbf{r})K(\mathbf{r})\psi(\mathbf{r})|^2}, \tag{22}$$

where

$$K(\mathbf{r})=|\mathbf{r}\rangle\langle\mathbf{r}|+\sum|\beta_n^I\rangle Q_{nm}^I(\mathbf{r})\langle\beta_m^I| \tag{23}$$

is the Vanderbilt density overlap operator. We find $p=0.22$ which indicates a rather delocalized state (for comparison, note that $p=0.003$ in the lowest occupied electronic state). We have also calculated the total probability for an electron in the LUMO to be within the spheres of radius $R_m=1.32$ Å centered around the O atoms. This turns out to be 28%. This number should instead be close to 0 if the σ^* were not contributing to the LUMO. A total volume of 32% is associated with the molecular spheres defined above. The difference between these two number measures the amount in which the LUMO states are actually expelled from the molecular region. Thus we find that our results based on a calculation for bulk water confirm those based on a cluster calculation.[60,61]

In support of the premise that the σ^* orbitals play no role, it is usually argued that in the molecule the σ^* orbitals have much too high an energy to be active (see, e.g., Ref. 56). Since in DFT the HOMO-LUMO gap can be underestimated by as much as a factor of 2, one could argue that DFT does not provide a sufficiently accurate description of one-electron properties such as electronic orbitals. However, DFT orbitals are in fact remarkably accurate in a large variety of systems. Furthermore quantum chemical calculations, where the HOMO-LUMO gap is much larger than ours, show the same effect, albeit quantitatively smaller. Regarding the objection that the HOMO-LUMO energy separation is too large to permit a sizable contribution of the molecular LUMO, it should also be mentioned that the zero (vacuum) level is likely to be localized in the middle of the HOMO-LUMO gap, hence the full gap need not be bridged.

A further argument of ours concerns the different conditions that prevail in the liquid as opposed to scattering from single molecules. The LUMO is necessarily orthogonal to all occupied orbitals, which implies that it must have σ^* character in the core region. The magnitude of the σ^* component is determined by how much the LUMO wave function tail penetrates the cores. In a condensed matter environment the overlap with the cores is enhanced by the strong confinement. This effect is illustrated by the dimer calculation where we have found that the LUMO is expelled from the H bond region. We believe this effect to be real. By reducing the accessible volume this effect will increase the energy of a hypothetical scattering state excluded from the inaccessible regions of space. This will bring the energy of this state to more closely match the energy of the σ^* molecular orbitals, thus favoring admixing.

VIII. DISCUSSION AND CONCLUSIONS

In this paper we have seen that the GC DF theory is capable of providing a satisfactory description of liquid water, although several questions remain to be addressed. The most crucial one is the role played by the choice of the gradient corrections. Better control of the properties of the GC is necessary, and this will require extensive testing. Another important issue to be discussed in the future is the equilibrium pressure in the *ab initio* water. Pressure has proved to be a rather severe test for classical model potentials.

We are also aware of the smallness of our system. The finite size effects can, however, be gauged from simulations that use classical potentials to verify that they are small for the first two peaks of the $g_{ij}(r)$ and are not responsible for the discrepancies between theory and experiment. Similarly the role of nuclear quantum corrections on the static properties has been discussed in the literature[63] and found to be small, especially in D_2O. Again we believe that this is

not a major source of discrepancy between theory and experiment.

Looking to future applications, we see that although the present results are rather encouraging, the computational costs of this calculation are still relatively high. It takes about one month on an IBM/RISC6000 model 550 to run the simulation for 1 ps. Thus progress must be made before one can use this methodology to study problems of solution chemistry for which the study of much larger systems is mandatory. However, rapid advances are being made in the development of new algorithms which either exploit parallel architectures[64] or have a much better scaling with system size.[65] This will soon allow us to study more complex chemical systems for which MD based on classical potentials presents severe difficulties, and to do so at computational costs that are affordable for many laboratories.

ACKNOWLEDGMENTS

We are indebted to David Vanderbilt for his crucial contributions to the development of the techniques applied to the present work. One of us (R.C.) acknowledges partial support from the Swiss National Science Foundation under Grant No. 21-3114491.

APPENDIX

In practical implementations of the GC energy density functional to *ab initio* molecular dynamics a considerable amount of numerical noise is observed which arises from the inaccuracies associated with the evaluation of the variable x_σ on a finite plane wave basis set. We have alleviated this problem by replacing $\rho(\mathbf{r})$ in the evaluation of $E_{\rm GC}$ with a smoothed density $\tilde{\rho}(\mathbf{r})$

$$E_{\rm xc}^{\rm GC}[\rho]=E_{\rm xc}^{\rm BP}[\tilde{\rho}],$$

where

$$\tilde{\rho}(\mathbf{r})=\sum_{\mathbf{G}}\rho_{\mathbf{G}}f(G)e^{-i\mathbf{G}\cdot\mathbf{r}}=\int d\mathbf{r}'\,g(\mathbf{r}-\mathbf{r}')\rho(\mathbf{r}'),$$
$$\nabla\tilde{\rho}(\mathbf{r})=-i\sum_{\mathbf{G}}\mathbf{G}\rho_{\mathbf{G}}f(G)e^{-i\mathbf{G}\cdot\mathbf{r}}, \tag{A1}$$

where $E_{\rm xc}^{\rm BP}$ denotes the Becke–Perdew form of GC, $\rho_{\mathbf{G}}$ is the Fourier transform of $\rho(\mathbf{r})$, and $f(\mathbf{G})$ is a smoothing function which we have taken of the Fermi type

$$f(G)=\frac{1}{1+\exp[(G-G_{\rm cut})/\Delta]}, \tag{A2}$$

and $g(\mathbf{r})$ is the convolution function corresponding to $f(\mathbf{G})$. In the present calculation the parameters of the Fermi function have been chosen as $G_{\rm cut}=0.9G_{\rm max}$ and $\Delta=0.8$. By introducing this smoothing procedure we have effectively redefined the GC energy. Thus the functional derivative of $E_{\rm xc}(\mu_{\rm xc})$ has to be consistent with the definition of $E_{\rm xc}$. Despite the nonlocal form of the $E_{\rm xc}$ the functional derivative can be determined without too much difficulty

$$\mu_{\rm xc}^{\rm GC}(\mathbf{r})=\frac{\delta E_{\rm xc}^{\rm BP}[\tilde{\rho}]}{\delta\rho(\mathbf{r})}$$
$$=\int d\mathbf{r}'\,\frac{\delta E_{\rm xc}^{\rm BP}[\tilde{\rho}]}{\delta\tilde{\rho}(\mathbf{r}')}\frac{\delta\tilde{\rho}(\mathbf{r}')}{\delta\rho(\mathbf{r})}$$
$$=\int d\mathbf{r}'\,\mu_{\rm xc}^{\rm BP}(\mathbf{r}')g(\mathbf{r}-\mathbf{r}')$$
$$=\sum_{\mathbf{G}}\mu_{\rm xc}^{\rm BP}(\mathbf{G})f(G)e^{-i\mathbf{G}\cdot\mathbf{r}}, \tag{A3}$$

where $\mu_{\rm xc}^{\rm BP}$ denotes the Becke–Perdew form of $\mu_{\rm xc}$.

This filtering procedure however does not fully eliminate all the sources of numerical noise. A good description of x_σ is still difficult to obtain in the very low charge density regions. These regions contribute very little to the total energy, yet due to large relative errors in $\rho(\mathbf{r})$ the integrand in Eq. (A1) can be locally rather large, leading to unphysically large fluctuations in $V_{\rm xc}(\mathbf{r})$. For these reasons we have decided to neglect all the GC contributions coming from regions where the density is below a threshold value. In the present calculation the threshold value is 8×10^{-4} e/(a.u.)^3; this value has to be compared with the $\rho(\mathbf{r})$ value hydrogen bond region of 0.03 e/(a.u.)^3. We have verified that these two corrections do not appreciably alter the values of the total energy nor the equilibrium geometries in calculations of small clusters.

[1] J. Caldwell, L. X. Dang, and P. A. Kollman, J. Am. Chem. Soc. **112**, 9145 (1990).
[2] M. Sprik, J. Chem. Phys. **95**, 6762 (1991).
[3] U. Niesar, G. Corongiu, E. Clementi, G. R. Kneller, and D. K. Bhattacharya, J. Phys. Chem. **94**, 7949 (1990).
[4] L. Perera and M. L. Berkowitz, J. Chem. Phys. **95**, 1954 (1991).
[5] M. Sprik, *Proc. Colloque Weyl VII*, edited by P. Damay and F. Leclercq, J. Phys. IV Colloque C **5**, 99 (1991).
[6] L. X. Dang, J. Chem. Phys. **97**, 2659 (1992).
[7] R. Car and M. Parrinello, Phys. Rev. Lett. **55**, 2471 (1985).
[8] G. Galli and M. Parrinello, in *Computer Simulations in Material Science*, edited by M. Meyer and V. Pontikis (Kluwer, Dordrecht, 1991), p. 283.
[9] R. Car and M. Parrinello, in *Simple Molecular Systems at Very High Density*, edited by A. Poliani, P. Loubeyre, and N. Boccara (Plenum, New York, 1989), p. 455.
[10] D. K. Remler and P. A. Madden, Mol. Phys. **70**, 921 (1990).
[11] M. C. Payne, M. P. Teter, D. C. Allan, T. A. Arias, and J. D. Joannopoulos, Rev. Mod. Phys. **64**, 1045 (1992).
[12] C. Lee, D. Vanderbilt, K. Laasonen, R. Car, and M. Parrinello, Phys. Rev. Lett. **69**, 462 (1992).
[13] C. Lee, D. Vanderbilt, K. Laasonen, R. Car, and M. Parrinello, Phys. Rev. B **47**, 4863 (1993).
[14] K. Laasonen, F. Csajka, and M. Parrinello, Chem. Phys. Lett. **194**, 172 (1992).
[15] K. Laasonen, M. Parrinello, R. Car, C. Lee, and D. Vanderbilt, Chem. Phys. Lett. **207**, 208 (1993).
[16] D. Vanderbilt, Phys. Rev. B **41**, 7892 (1990).
[17] A. D. Becke, Phys. Rev. A **38**, 3098 (1988); J. Chem. Phys. **96**, 2155 (1992).
[18] J. P. Perdew, Phys. Rev. B **33**, 8822 (1986).
[19] K. Laasonen, R. Car, C. Lee, and D. Vanderbilt, Phys. Rev. B **43**, 6796 (1991).
[20] K. Laasonen, A. Pasquarello, R. Car, C. Lee, and D. Vanderbilt, Phys. Rev. B **47**, 10142 (1993).
[21] R. N. Barnett and U. Landman, Phys. Rev. Lett. **70**, 1775 (1993).
[22] A. Migus, Y. Gauduel, J. L. Martin, and A. Antonetti, Phys. Rev. Lett. **58**, 1559 (1987).

[23] F. H. Long, H. Lu, and K. B. Eisenthal, Phys. Rev. Lett. **64**, 1469 (1990).
[24] M. C. Messmer and J. D. Simon, J. Phys. Chem. **94**, 1220 (1990); Phys. Rev. Lett. **64**, 1469 (1990).
[25] P. J. Rossky and J. Schnitker, J. Phys. Chem. **92**, 4277 (1988).
[26] F. J. Webster, J. Schnitker, M. S. Friedrichs, R. A. Friesner, and P. J. Rossky, Phys. Rev. Lett. **66**, 3172 (1991); F. J. Webster, P. J. Rossky, and R. A. Friesner, Comput. Phys. Commun. **63**, 494 (1991).
[27] M. L. Cohen and J. R. Cheliskowsky, *Electronic Structure and Optical Properties of Semiconductors* (Springer, Berlin, 1988), p. 16; W. E. Picket, Comp. Phys. Rep. **9**, 115 (1989).
[28] D. R. Hamann, M. Schlüter, and C. Chiang, Phys. Rev. Lett. **43**, 1494 (1979), G. B. Bachelet, D. R. Hamann, and M. Schlüter, Phys. Rev. B **26**, 4199 (1982).
[29] A. M. Rappe, K. M. Rabe, E. Kaxiras, and J. D. Joannopoulos, Phys. Rev. B **41**, 1227 (1990).
[30] N. Troullier and J. L. Martins, Phys. Rev. B **43**, 1993 (1991).
[31] P. Blöchl, Phys. Rev. B (submitted).
[32] O. K. Anderson, Phys. Rev. B **12**, 3060 (1975).
[33] J. P. Ryckaert, G. Ciccotti, and H. J. C. Berendsen, J. Comput Phys. **23**, 327 (1977); G. Ciccotti and J. P. Ryckaert, Comput. Phys. Rep. **4**, 345 (1986).
[34] O. Gunnarson and R. D. Jones, Rev. Mod. Phys. **61**, 689 (1991).
[35] J. Perdew and A. Zunger, Phys. Rev. B **23**, 5048 (1981).
[36] D. M. Ceperley and B. J. Alder, Phys. Rev. Lett. **45**, 566 (1980).
[37] G. Ortiz and P. Ballone, Phys. Rev. B **43**, 6376 (1991).
[38] J. P. Perdew, J. A. Chevary, S. H. Vosko, K. A. Jackson, M. R. Pederson, D. J. Singh, and C. Fiolhais, Phys. Rev. B **46**, 6671 (1992).
[39] A. Garcia, C. Elaesser, J. Zhu, S. G. Louie, and M. L. Cohen, Phys. Rev. B **46**, 9829 (1992); **47**, 4150 (1993).
[40] W. L. Jorgensen, J. Chandrasekhar, J. D. Madura, R. W. Impey, and M. L. Klein, J. Chem. Phys. **79**, 926 (1983).
[41] A. K. Soper and M. G. Philips, Chem. Phys. **107**, 47 (1986).
[42] K. Krynicki, C. D. Green, and D. W. Sawyer, Faraday Discussion Chem. Soc. **66**, 199 (1978).
[43] G. E. Walrafen, in *Water, A Comprehensive Treatise*, edited by F. Franks (Plenum, New York, 1971).
[44] K. Toukan, M. A. Ricci, S.-H. Chen, C.-K. Loong, D. L. Price, and J. Teixeira, Phys. Rev. A **37**, 2580 (1982).
[45] E. Honegger and S. Leutwyler, J. Chem. Phys. **88**, 2582 (1988); R. Knochenmuss and S. Leutwyler *ibid.* **96**, 5233 (1992).
[46] K. S. Kim, M. Dupuis, G. C. Lie, and E. Clementi, Chem. Phys. Lett. **131**, 451 (1986).
[47] K. Laasonen, M. Sprik, and M. Parrinello, *Proc. Int'l Workshop on Ultrafast Reaction Dynamics and Solvent Effects, Abbaye de Royaumont, France, May 12–14, 1993* (AIP, New York, 1993).
[48] A. C. Shepard, Y. Beers, G. P. Klein, and L. S. Rothman, J. Chem. Phys. **59**, 2254 (1973).
[49] C. A. Coulson and D. Eisenberg, Proc. R. Soc. London, Ser. A **291**, 445 (1966).
[50] T. Shibaguchi, H. Onuki, and R. Onaka, J. Phys. Soc. Jpn. **42**, 152 (1977).
[51] K. Kimura, S. Katsumate, Y. Achiba, T. Yamazaki, and S. Iwata, *Handbook of HeI Photoelectron Spectra of Fundamental Organic Molecules* (Japan Scientific Society, Tokyo, 1981).
[52] B. J. Rosenberg and I. Shavitt, J. Chem. Phys. **63**, 2162 (1975).
[53] G. Pastori Parravicini and L. Resca, Phys. Rev. B **8**, 3009 (1973).
[54] B. Baron, D. Hoover, and F. Williams, J. Chem. Phys. **68**, 1997 (1978).
[55] D. Grand, A. Bernas, and E. Amouyal, Chem. Phys. **44**, 73 (1979).
[56] J. Schnitker and P. J. Rossky, J. Chem. Phys. **86**, 3462 (1987).
[57] A. Wallqvist, D. Thirumalai, and B. J. Berne, J. Chem. Phys. **86**, 6404 (1987); A. Wallqvist, G. Martyna, and B. J. Berne, J. Phys. Chem. **92**, 1721 (1988).
[58] R. N. Barnett, U. Landman, C. L. Cleveland, and J. Jortner, J. Chem. Phys. **88**, 4421, 4429 (1988); R. N. Barnett, U. Landman, G. Makov, and A. Nitzan, *ibid.* **93**, 6226 (1990).
[59] M. Sprik, J. Phys. Condens. Matter **2**, SA161 (1990).
[60] M. D. Newton, J. Phys. Chem. **79**, 2795 (1975).
[61] T. Clark and G. Illing, J. Am. Chem. Soc. **109**, 1013 (1987); A. E. Read and T. Clark, Faraday Discuss. Chem. Soc. **85**, 365 (1988).
[62] S. Schlick, P. A. Narayana, and L. Kevan, J. Chem. Phys. **64**, 3153 (1976).
[63] R. A. Kuharski and P. J. Rossky, J. Chem. Phys. **82**, 5164 (1985).
[64] I. Stich, M. C. Payne, R. D. King-Smith, J.-S. Lin, and L. J. Clarke, Phys. Rev. Lett. **68**, 1351 (1992).
[65] G. Galli and M. Parrinello, Phys. Rev. Lett. **69**, 3547 (1992).